ELSEVIER

Journal of Nuclear Materials 258–263 (1998) 1817–1821

journal of nuclear materials

Radiation effects on Al_2O_3 irradiated with H_2^+ ions

S. Furuno [a,*], N. Sasajima [b], K. Hojou [a], K. Izui [a], H. Otsu [a], T. Matsui [b]

[a] *Department of Materials Science and Engineering, Japan Atomic Energy Research Institute, Tokai-mura, Ibaraki-ken 319-1195, Japan*
[b] *Department of Quantum Engineering, Nagoya University, Chikusa, Nagoya, Aichi 464, Japan*

Abstract

In situ electron microscope observations were performed to investigate damage evolution in Al_2O_3 single crystals during H_2^+ ion irradiations in an electron microscope linked with an ion accelerator. The irradiations were made with 15 keV H_2^+ ions for 1 h at a flux of 1×10^{18} H/m^{2}s at room temperature, 400°C, 650°C and 800°C. It was observed that there were two temperature ranges characteristic of behaviors of the formation and growth of defect clusters. In the lower temperature range below 400°C, dislocation loops and bubbles were formed uniformly. In the higher temperature range above 650°C, bubbles were formed with the dislocation loops almost at the same time, and they located preferentially inside the planes of the dislocation loops. As the irradiation proceeded, the number of bubbles inside the loops increased with the loop growth, but the size of bubbles hardly changed. These observation results seem to indicate that the formation and growth of the bubbles are promoted by the defects on loop planes in a high temperature range.

1. Introduction

Alumina (Al_2O_3) is considered to be one of the important candidate ceramics materials for various components in fusion reactors such as the window for a microwave heating system and a insulating material [1]. These plasma facing ceramics will be subject to intense irradiations with energetic neutrons and ions. Therefore it is important to clarify radiation damages in these ceramics caused by neutrons, protons, α-particles and other ion species. To evaluate the potentials for the applications, it is important to estimate dimensional changes and degradation in electrical properties and thermal conductivity of these ceramics.

From a standpoint of application, triple ion irradiation experiments have been performed to examine multiple effects under a condition closer to that of practical fusion reactors [2]. Single ion irradiation experiments on the specimens pre-implanted with helium or hydrogen ions have also been performed to examine the synergistic effects of transmutation products [3–5]. To understand the irradiation effects observed under the complicated irradiation conditions mentioned above, it is important to accumulate precise and reliable data obtained under simplified irradiation conditions with a single ion beam.

From a fundamental standpoint, on the other hand, Al_2O_3 is an interesting material because Al_2O_3 shows unique features in damage productions. For example, it has been reported that one-dimensional arrays of voids aligned along ⟨0 0 0 1⟩ direction were observed under neutron irradiations [6,7] and heavy ion irradiations [3,4], and that dislocation loop formation was suppressed under a high energy light ion irradiation, as observed in the case of $MgAl_2O_4$ [8]. Up to now, many investigations on the irradiation damage have been carried out with Al_2O_3, but hydrogen ion irradiation effects on Al_2O_3 have been reported only a little.

In this paper, we report the results of in situ electron microscope observations on the damage evolution in Al_2O_3 during hydrogen ion irradiations.

2. Experimental procedure

Specimens used here were 0.5 mm thick single crystal wafers of α-Al_2O_3 whose surfaces are parallel to the (0 0 0 1) hexagonal plane. Both sides of these specimens were polished with diamond paste and discs with a

* Corresponding author. Tel.: +81 29 2826360; fax: +81 29 2826716.

0022-3115/98/$19.00
PII: S0022-3115(98)00408-5

diameter of 3 mm were cut off from these wafers by an ultrasonic cutter. Then discs were dimpled to a thickness of 20 μm at the center using a dimpling machine. Perforation was achieved in the dimpled region by etching with 3 keV Ar^+ ions at an incident angle of 20° to the surface of discs. Final polishing was carried out with 2 keV ions at 15°. These thinning procedures were performed at an ambient temperature. All the specimens were annealed at 1100°C for 10 h in the air in order to remove the defects introduced during ion thinning procedures.

Irradiation experiments were performed in an electron microscope (JEM-2000F) linked with an ion accelerator. The ion beam was incident to the specimen surface at an angle of 60°. The beam was of 15 keV H_2^+ ions with a flux of 5×10^{17} H_2^+/m^2s, which corresponds to single H ions with an average energy of 7.5 keV with a flux of 1×10^{18} H/m^2s. This ion energy was decided from TRIM-code calculations in which displacement threshold energies of 24 eV for aluminum sublattice and 78 eV for oxygen sublattice were adopted, respectively [8]. The calculation results showed that the implanted ions had a projection range of 130 nm with a peak concentration at a depth of 70 nm and 90% of the implanted ions rested in the specimens with the thickness of 100 nm. The displacement damage peak was 0.75 dpa at the depth of 60 nm at the fluence of 3.6×10^{21} H/m^2. The irradiations were carried out at room temperature, 400°C, 650°C and 800°C. Each specimen was heated during the irradiations using a single-tilt-type Gatan hot stage. All the irradiations were carried out for one hour. The final fluence of all the irradiations reached 3.6×10^{21} H/m^2.

3. Results and discussion

It seems better to show the results classifying into two irradiation temperature ranges, below 400°C and above 650°C, because the behavior in the formation and the growth of defect clusters and bubbles was characteristic in these two temperature ranges.

3.1. Irradiations at room temperature and 400°C

Fig. 1 shows the damage evolution in Al_2O_3 during H_2^+ ion irradiation at room temperature. Small defect clusters with weak contrast were homogeneously formed at an early stage of the irradiation at a fluence less than 6×10^{19} H/m^2. The number density of the defect clusters increased with the increasing fluence up to 6×10^{20} H/m^2, and then stopped to increase. The defect clusters grew in size with the increasing fluence up to 1.2×10^{21} H/m^2. Beyond this fluence the growth of defect cluster size was not apparent.

Bubbles were homogeneously formed at the fluence less than 1.2×10^{21} H/m^2. The number density of the bubbles increased with the increasing fluence. Beyond the fluence of 2.7×10^{21} H/m^2 some bubbles turned into string-like defects by coalescence with each other.

Fig. 2 shows the damage evolution in Al_2O_3 during H_2^+ ion irradiation at 400°C. Defect clusters were homogeneously formed at a fluence less than 3×10^{19} H/m^2. The number density of the defect clusters increased with the increasing fluence up to 6×10^{20} H/m^2. Beyond this fluence the increment of the number density was suppressed. The defect clusters grew in size with the increasing fluence up to 1.8×10^{21} H/m^2. Beyond this fluence growth of defect clusters was not observed.

Bubbles were homogeneously formed in a fluence of 6×10^{20} H/m^2. The number density of bubbles increased with the increasing fluence up to 1.8×10^{21} H/m^2 and then the increment of the number density was suppressed. The bubbles grew in size with the increasing fluence. At the fluence of 3.6×10^{21} H/m^2 the diameter of the bubbles reached about 3 nm.

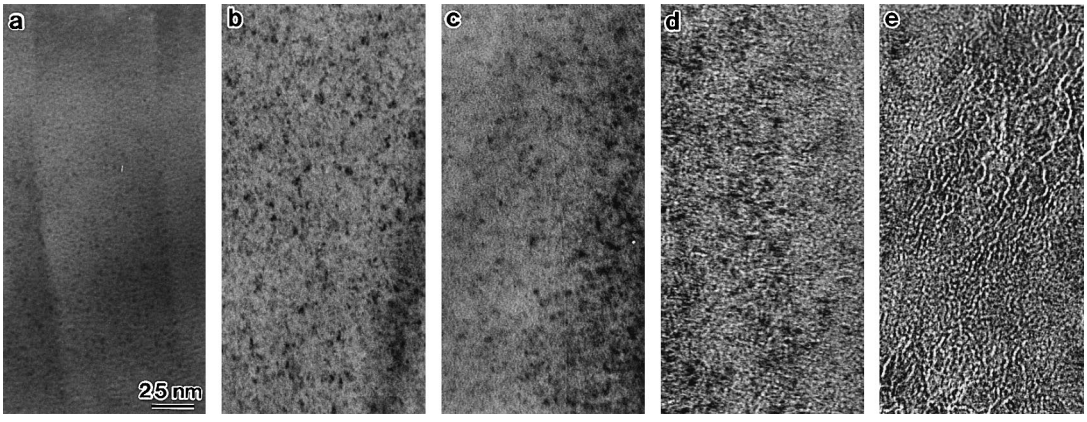

Fig. 1. TEM images of (0 0 0 1) plane of Al_2O_3 during 15 keV H_2^+ ion irradiation at room temperature. (a) 6×10^{19} H/m^2, (b) 6×10^{20} H/m^2, (c) 1.2×10^{21} H/m^2, (d) 2.7×10^{21} H/m^2, (e) 3.6×10^{21} H/m^2.

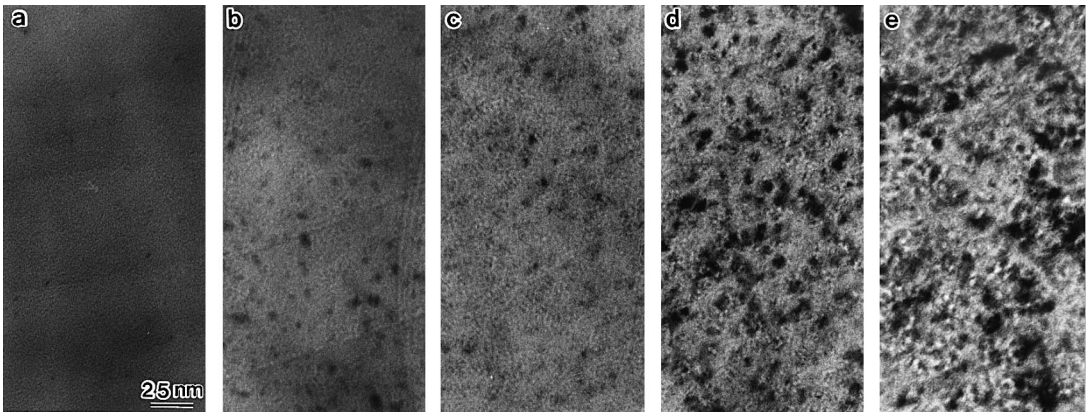

Fig. 2. TEM images of (0 0 0 1) plane of Al_2O_3 during 15 keV H_2^+ ion irradiation at 400°C. (a) 3×10^{19} H/m^2, (b) 1.8×10^{20} H/m^2, (c) 6×10^{20} H/m^2, (d) 1.8×10^{21} H/m^2, (e) 3.6×10^{21} H/m^2.

These results indicate that the higher the irradiation temperature is, the earlier the defect clusters are formed, as is shown in Fig. 1 (a) and 2 (a) and that bubbles are formed, on the other hand, later than loops as shown in Fig. 1(a)–(c) and Fig. 2(a)–(c).

3.2. Irradiations at 650°C and 800°C

Fig. 3 shows the damage evolution in Al_2O_3 during H_2^+ ion irradiation at 650°C. Dislocation loops were observed at a fluence of 1.8×10^{20} H/m^2. These loops were accompanied with planar and seemingly linear arrays of small bubbles as shown in Fig. 3(a). These loop planes were confirmed to be $(1\,0\,\bar{1}\,0)$, $(\bar{1}\,1\,0\,0)$, $(0\,1\,\bar{1}\,0)$, and (0 0 0 1) planes by the diffraction patterns. The number and the size of loops increased and became tangled with the increasing fluence. Bubbles were formed preferentially inside the planes of the dislocation loops. The number of bubbles increased with the increasing fluence up to 6×10^{20} H/m^2. Beyond this fluence the increment of the number of bubbles became less clear because of the complicated contrast induced by tangled dislocations. It was observed that these bubbles grew little in size with a constant diameter of about 2 nm up to the fluence of 6×10^{20} H/m^2. Some bubbles in the region of tangled loops, however, were observed to grow up to the diameter of about 10 nm at the fluence of 3.6×10^{21} H/m^2.

Fig. 4 shows the damage evolution in Al_2O_3 during H_2^+ ion irradiation at 800°C. Dislocation loops were observed at a fluence of 3×10^{20} H/m^2. These loops were accompanied with planar and seemingly linear arrays of small bubbles as shown in Fig. 4(a). These loop planes were confirmed to be $(1\,0\,\bar{1}\,0)$, $(\bar{1}\,1\,0\,0)$, $(0\,1\,\bar{1}\,0)$, and (0 0 0 1) planes by the diffraction patterns. In addition, the loops grew also on three other planes: $(\bar{1}\,2\,\bar{1}\,0)$, $(1\,1\,\bar{2}\,0)$ and $(\bar{2}\,1\,1\,0)$, as shown with arrows in Fig. 5. The number and the size of the loops increased

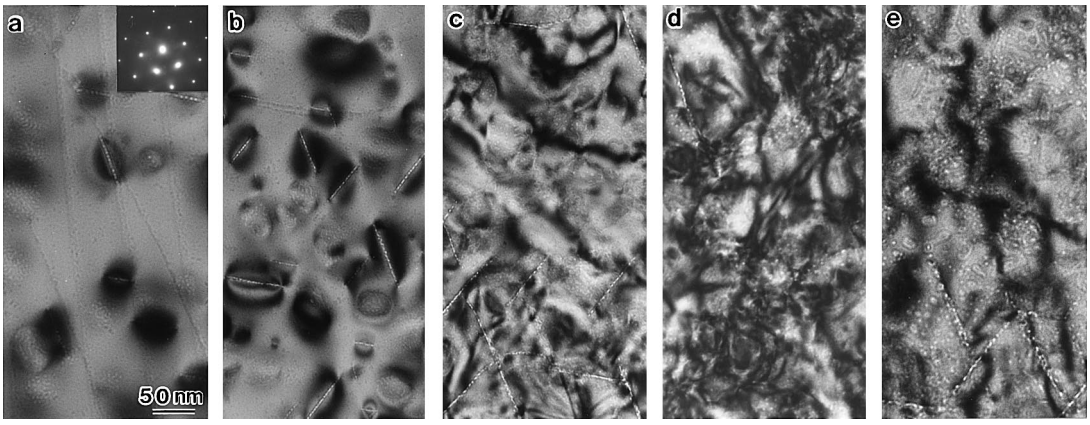

Fig. 3. TEM images of (0 0 0 1) plane of Al_2O_3 during 15 keV H_2^+ ion irradiation at 650°C. (a) 1.8×10^{20} H/m^2, (b) 3×10^{20} H/m^2, (c) 6×10^{20} H/m^2, (d) 1.8×10^{21} H/m^2, (e) 3.6×10^{21} H/m^2.

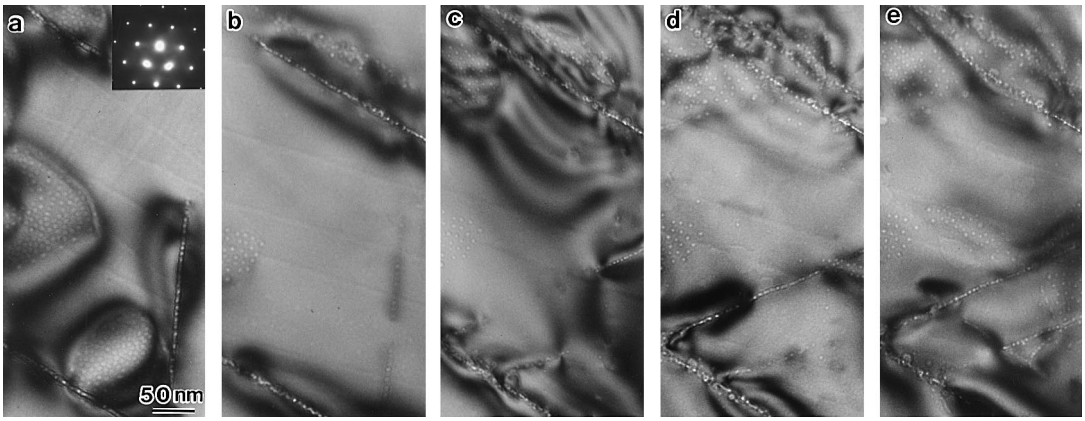

Fig. 4. TEM images of (0 0 0 1) plane of Al_2O_3 during 15 keV H_2^+ ion irradiation at 800°C. (a) 3×10^{20} H/m^2, (b) 6×10^{20} H/m^2, (c) 1.8×10^{20} H/m^2, (d) 2.7×10^{21} H/m^2, (e) 3.6×10^{21} H/m^2.

a little with the increasing fluence. Bubbles were formed preferentially inside the planes of the dislocation loops. The number of bubbles increased a little with the increasing fluence. It was observed that these bubbles grew little in size with a constant diameter of about 4 nm. Some bubbles, however, trapped on the dislocation lines were observed to grow up to the diameter of about 10 nm at a fluence of 3.6×10^{21} H/m^2.

A remarkable feature observed in the present experiments is that bubbles were formed uniformly in the lower temperature range from room temperature to 400°C, while in the higher temperature range from 650°C to 800°C bubbles were formed heterogeneously, that is, formed preferentially in the loop planes.

This phenomenon can be explained by considering the behavior of interstitial atoms and vacancies produced by the ion irradiations. In the relatively low temperature range below 400°C, large part of interstitial atoms may escape to the surface of the thin specimen. Some of them will annihilate by combining with va-

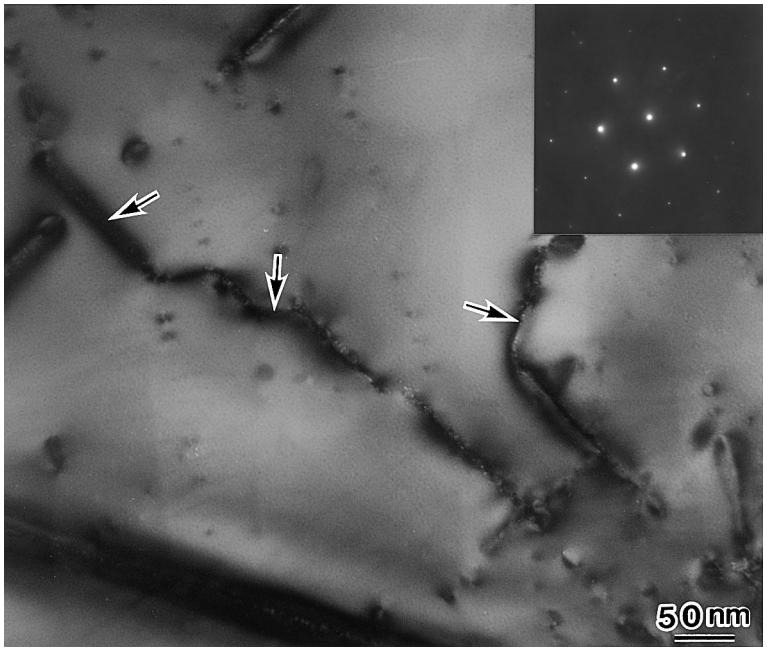

Fig. 5. TEM images of (0 0 0 1) plane of Al_2O_3 taken to examine loop habit planes. The specimen were irradiated with 15 keV H_2^+ ions to a fluence of 3.6×10^{21} H/m^2 at 800°C. In addition to (1 0 $\bar{1}$ 0), ($\bar{1}$ 1 0 0), (0 1 $\bar{1}$ 0) and (0 0 0 1) planes, ($\bar{1}$ 2 $\bar{1}$ 0), (1 1 $\bar{2}$ 0) and ($\bar{2}$ 1 1 0) planes marked with arrows are observed.

cancies, while the rest of them will cluster to form small interstitial loops. As the vacancies move slowly than interstitial atoms, they cluster with each other after the formation of the interstitial loops.

In the high temperature range above 650°C, homogeneous nucleation of bubbles seems difficult in other places than loop planes because the probability of decomposition of divacancies or small vacancy clusters is high, even if they are instantaneously formed. On the other hand, interstitial loops in Al_2O_3 have a complicated structure consisting of 4 layers extraplanes [6]. In the growing process of these interstitial loops some defects will possibly be left at some points in the loop planes. These defects will act as effective trapping centers for vacancies and for hydrogen atoms, which can be stable nuclei for the bubble formation. Moreover, dislocations have bias effects due to strain field, that is, they are apt to absorb interstitial atoms rather than vacancies. As a result, in the vicinity of the dislocations, the density of vacancies become high, which is favorable for the formation of small bubbles. The points mentioned above account for the preferential formation of small bubbles in the loop planes.

4. Conclusion

In the lower temperature range dislocation loops and bubbles were formed uniformly. In the higher temperature range, on the other hand, small bubbles were formed heterogeneously, that is, formed preferentially in the loop planes. This heterogeneous formation of bubbles seems to be promoted by trapping of vacancies and hydrogen atoms to the defects in the loop planes and the rise of vacancy concentration by bias effect of dislocations. In this case, the higher the irradiation temperature was, the later dislocation loops and bubbles were formed.

Acknowledgements

One of the authors (N.S) has been supported by the Research Fellowships of the Japan Society for the Promotion of Science for Young Scientists.

References

[1] F.W. Clinard, Jr., G.F. Hurley, R.W. Klaffky, Res. Mechanica 8 (1983) 207.
[2] Y. Katano, T. Nakazawa, D. Yamaki, T. Aruga, K. Noda, J. Nucl. Mater. 233–237 (1996) 1325.
[3] W.E. Lee, G.P. Pells, M.L. Jenkens, J. Nucl. Mater. 122–123 (1984) 1393.
[4] W.E. Lee, M.L. Jenkens, Philos. Mag. A 51 (5) (1985) 639.
[5] R. Yamada, S.J. Zinkle, G.P. Pells, J. Nucl. Mater. 209 (1994) 191.
[6] F.W. Clinard Jr., G.F. Hurley, L.W. Hobbs, J. Nucl. Mater. 108&109 (1982) 655.
[7] R.A. Youngman, T.E. Mitchell, F.W. Clinard Jr., G.F. Hurley, J. Mater. Res. 6 (10) (1991) 2178.
[8] S.J. Zinkle, J. Nucl. Mater. 219 (1995) 113.